





Application of Pass-Band Step Filtering Method for Identification the Vibration-Acoustic Signature of a Moving Train

Rafał Burdzik^(✉)  and Paweł Słowiński 

Faculty of Transport and Aviation Engineering, Silasian University of
Technology, Krasińskiego 8, 40-019 Katowice, Poland
{rafal.burdzik,pawel.slowinski}@polsl.pl

Abstract. The paper presents research on application of pass-band step filtering method for identification the vibration-acoustic signature of a moving train. Authors present results of applying new methods of filtering vibration-acoustic signatures. The signal comb filtering was applied and the RMS in the time course and the sum of the FFT amplitudes in the spectra were used as a general measure after filtering the signal. Modern rail vehicles, as well as those modernized due to reaching high speed (HSR), arouse interest in terms of vibration and acoustic signals that they generate, especially in the context of the changing market of rail transport services in Central Europe. Rail transport and railway infrastructure managers perceive the problem of acoustic comfort in the vicinity of railway routes, therefore this subject becomes an important aspect from the point of view of further analyzes. The issue of the use of various filtering methods to identify the vibration and acoustic signature of a moving train is of key importance for further analyzes of research on environmental comfort as well as other research on vibroacoustic signals on the railway.

Keywords: Vibration · Noise · Train · Vibroacoustic signature

1 Introduction

1.1 Vibrations and Noise of Railway Trains - Classification of Random Signals

The classification of vibrations coming from all means of transport is classified as random-non-stationary paraseismic vibrations. Signals corresponding to random physical phenomena cannot be described with exact mathematical relationships, because the result of each observation of a signal is the only one (non-reproducible). A single time function describing a random phenomenon is called a random function or an execution, and at a finite time interval - an observed signal [5].

Four statistical functions are used to describe the main properties of random signals:

- Mean square value.
- Probability density function.

- Autocorrelation function.
- Power spectral density function.

The higher vibrations occur when the excitation frequency is close to the natural frequency of the vehicle rail-track system [1, 2, 15]. This pseudo-resonance phenomena is important for vibration analysis. Especially when vibroacoustic signature is analysed and other parameters of the signal related with train dynamics and types are investigated [11]. The dominant source of noise from the low velocity moving train set is the rotating wheel of the trolley on the rail, and more precisely the wheel-rail contact mechanism, which depends on the speed and unevenness of the running surfaces or damage [3, 4, 6, 16–18].

Many of papers focus on the problem of noise generated by moving rail vehicles [9]. The sources of external noise emitted by rolling stock are listed below [10, 14]:

- a) primary noise - noise during rolling stock movement,
- b) basic - caused by the wheel rolling on the rail,
- c) other factors - noise from traction and auxiliary machinery, air turbulence, noise generated by pantographs and vibrations of individual vehicle parts,
- d) secondary - signals from the locomotive, noise from manoeuvres.

There are three basic categories of noise sources in moving trains: traction noise, rolling noise and aerodynamic. At a train speed of up to 30 km/h, the noise emitted by the vehicle itself, e.g. a working diesel engine, is the most important. Above 30 km/h to 200 km/h, the main source of noise is the noise caused by rolling of wheel on the rail causing all rail-wheel contact phenomenon. However, aerodynamic noise is the main source of noise only above 200 km/h, i.e. for HSR passenger trains. Below approx. 70 km/h the aerodynamic noise is below 70 dB (A).

In the case of rail vibrations, the problems are different than in the case of wheel vibrations [7, 8, 12]. The rail has a different characteristic in which the wave is supported and spreads along its entire length.

To sum up, from the point of view of the operation of means of railway transport, the most important sources of vibrations include:

- contact phenomena in the wheel-rail system;
- operation of the drive unit;
- air vibrations when the vehicle is in motion;
- effects of unbalance of mechanical parts in vehicles.

1.2 Research Problem and Research Method

The authors formulated new research goals as the analysis of synchronized vibroacoustic images in the aspect of assessing the information capacity of the recorded signals. This forced an increase in the scope of research and continuation of the currently conducted research and experiments. The research method was developed, the assumption of which was the synchronous registration of acoustic signals in the immediate vicinity of the track and vibrations in three directions recorded directly on the rail. The signals were recorded by the LabVIEW software.

The measurement system used for this research included:

- Three Endevco accelerometers with the following parameters: Sensitivity: 100 mV/g | 10.2 mV/m/s², maximum measuring range: 50 g pk | 491 m/s² pk. Sampling rate 42,000 Hz;
- Data acquisition module: 24 bits max 50 kHz;
- Integrating sound level meter SON-50 type with accuracy class 1 and measuring range in dB in 4 sub-ranges.

The accelerometers were attached to the special metal cube and by the magnets to the rail (on the web). However, tests are also possible on the foot of the rail [13]. The signal was recorded in three orthogonal axes X, Y, Z, where the X axis (along the track axis), the Y axis (transversely to the track axis), and the Z axis (vertical to the track axis). The ambient temperature was 6 degrees Celsius. An example of the mounting method (mounting through a magnet attached to the rail) is shown in the graphic below.

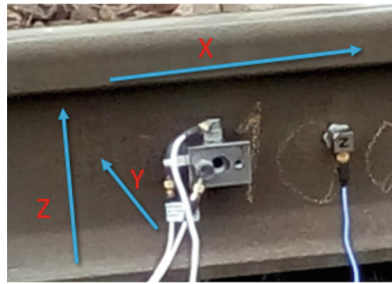


Fig. 1. The method of mounting the sensor to the rail. Own source.

2 Methods of Analysis

The authors used a band-pass filter - an algorithm that passes the spectral components of the signal in a specific frequency range, called the passband. The bandwidth of a bandpass filter is defined as the range between the low f_L and upper f_H cut-off frequency, or as a range around a specific center frequency of this filter. The relationship between the cutoff frequencies and the center frequency and bandwidth B is expressed by the formulas:

$$f_0 = \sqrt{f_L f_H},$$

$$B = f_H - f_L.$$

The filtering range was from 100 Hz to 2,400 Hz in 100 Hz steps. The signal processing contain pass-band filtering 100–200 Hz, waveform analysis (RMS), FFT analysis and the spectrogram. The scheme of the procedure is presented below:

- Performing vibration measurements in three axes.
- Performing noise measurements.

- Selecting from the course of vibrations and noise the fragments related to the passage over the sensor.
- Prior to filtering, categorized into four categories of trains.
- Analysis of unfiltered signals and determination of the “boundary” for the performance of the bandpass filter.
- Running a script in a MATLAB environment containing a band-pass filter, e.g. 0 to 2,400 Hz in 100 Hz intervals.
- The saved files after filtering are subjected to further analysis, e.g. RMS, FFT determination.
- After performing the FFT analysis in a given frequency range, the maximum values $|dft(f)|$ are determined and rewrites to the table.
- The written values from the table are ready to be presented in the form of graphs and compared to each other.

The correct operation of the filter with a slight transmission within its operating limits can be noticed, which is confirmed by the FFT analysis as well as the spectrogram.

The recording of vibrations and noise was performed synchronously. Also the correct operation of the filter with slight transmission within its operating limits can be confirmed, which is confirmed by the FFT analysis as well as the spectrogram. Higher values related to the filter pass-through were noticed at frequencies above 5,000 Hz.

3 Results

3.1 Vibration Measurements

The results were recorded on the railway route located in Poland, on the main railway line on the Wrocław-Katowice section. Due to the variety of measurement points in which the authors made the measurements, the focus was only on those carried out at one point, on the same day, with the same weather and environmental conditions. The characteristics of the trains are:

- Electric multiple unit (EMU) - 120 km/h - Quantity of car numbers: 3 – Railcar.
- High-speed rail (HSR) – 160 km/h - Quantity of car numbers: 8.
- Electric locomotive with passenger railroad cars (PO) – 120 km/h - Quantity of car numbers: 4.
- Electric locomotive with hopper wagons (TO) – 60 km/h - Quantity of car numbers 41.

The vibration signals of vehicles differs significantly in various respects, but the most important of them include, first of all, the length of the train (and the time of its registration depending on the speed of the train - in this case the speed of the EMU, HSR and PO trains was higher) than cut on the trail due to the measurements on the main bus the number of amplification of the signal (indicating the wheel passing over the sensor). The amplitude in the course of the above-mentioned trains has the greatest gain in the Electric locomotive with hopper wagons and Electric locomotive with

passenger railroad cars (TO, PO) compositions, while the ED250 (HSR) composition has the lowest (Table 1).

Table 1. Calculated RMS, Peak 2 Peak and Max values for the waveforms before filtering.

Type	RMS	PEAK 2 PEAK	MAX value
Electric multiple unit (EMU)	8,326	112,8	56,39
High-speed rail (HSR)	2,476	65,20	33,50
Electric locomotive with passenger railroad cars (PO)	11,201	112,8	56,39
Electric locomotive with hopper wagons (TO)	3,821	108,1	51,66

Also in the case of the FFT analysis for the X axis of unfiltered signals, differences in gain levels for given frequencies can be noticed. A characteristic feature is the fact that the gains are up to 2,500 Hz, which also takes place in further analysis using a band-pass filter at frequencies from 100 Hz to 2,500 Hz every 100 Hz.

Summary of the results after filtering, taking into account the highest amplitude value for a given analysed frequency with the bandpass filter 100–2,400 Hz (Fig. 2).

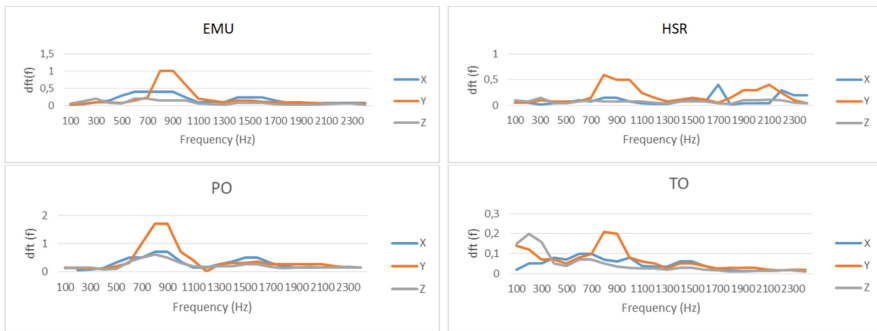


Fig. 2. Results after filtering with the band-pass step method in the range from 100 to 2,400 Hz in 100 Hz windows - the highest amplitude. Y axis - gain, X axis - frequency (Hz). The axes are designated X Y Z (see at Fig. 1). Results for EMU. Values from the signal spectra.

For EMU the highest value of the spectrum can be noticed for frequencies from 700 to 1,100 Hz, especially around 900 Hz where this value reaches 1. However, the X and Z axes are characterized by a lower gain, while for the X axis this gain of 0.4 and 0.3 is found in the ranges of 600–900 Hz and 1,400–1,600 Hz. In the Z axis, no significant reinforcements are found (the highest value 0.2). For High Speed Railways, the highest value of the spectrum can be noticed for frequencies from 700 to 1,150 Hz, especially around 800 Hz where this value reaches 0.6 and in frequencies between 1,900–2,300 Hz. On the other hand, the X and Z axes are characterized by a lower gain, while

for the X axis the gain of 0.4 and 0.3 is found in the 1,600–1,800 Hz and 2,200 Hz ranges. In the Z axis, no significant reinforcements are found (the highest value of 0.15). For Electric locomotive with passenger railroad cars, the highest value of the spectrum can be noticed for frequencies from 600 to 1,150 Hz, especially around 800–900 Hz, where this value reaches 1.7. On the other hand, the X and Z axes are characterized by a lower gain, while for the X axis the gain of 0.7 and 0.5 is found in the 600–1,000 Hz and 1,500–1,600 Hz ranges. In the Z axis, the highest value was found between 700–900 Hz for a value of approx. 0.5. For a freight train, the highest value of the spectrum can be noticed for frequencies up to 300 Hz and from 750 to 1,000 Hz, where this value is 0.15 and 0.2 respectively. On the other hand, the X and Z axes are characterized by a lower gain, while for the X axis the gain of 0.05 to 0.1 is found in the 400–800 Hz ranges. In the Z axis, the highest value was found for the frequency of about 250 Hz for the value of 0.2.

The following statement of results after filtering takes into account the RMS values for a given analyzed frequency using the Bandpass 100–2,400 Hz filter (Fig. 3).

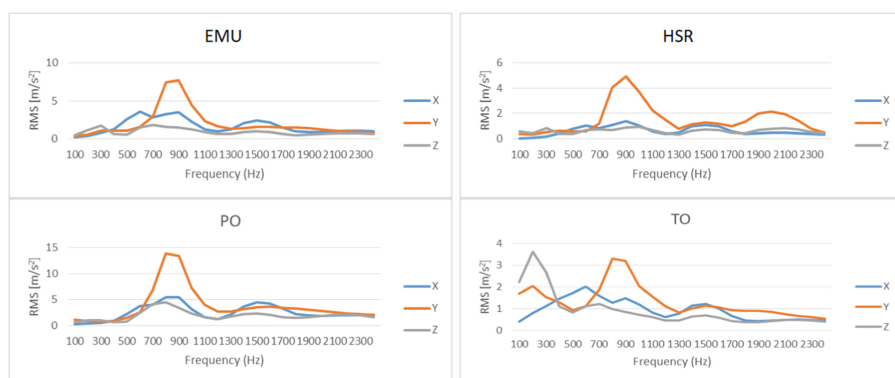


Fig. 3. Results after band-pass step method filtering in the range from 100 to 2,400 Hz in 100 Hz windows. The axes are designated X Y Z (see at Fig. 1). Results for EMU. Determined RMS values for given frequencies.

For EMU, the highest RMS value can be noticed for frequencies from 700 to 1,100 Hz in the Y axis, especially around 800–900 Hz where this value reaches approx. 7. The X and Z axes are characterized by lower RMS values, but for the X axis these values are not more than 3.5 for 600 Hz. In the Z axis, the highest value was found for 700 Hz and it amounts to 2. For HSR, the highest RMS value can be noticed for frequencies from 700 to 1,100 Hz in the Y axis, especially for 900 Hz where this value reaches 5. However, the X and Z axes are characterized by smaller RMS values, but for the X axis these values are no more than 1, 2 for 900 Hz. In the Z axis, the highest value was found for 1,000 Hz and it amounts to 1. For the PO, the highest RMS value can be noticed for the frequencies from 700 to 1,000 Hz in the Y axis, especially around 800–900 Hz where this value reaches approx. 14. The X and Z axes are characterized by smaller RMS values, but for the X axis these values are not more than 6 in the range 800–900 Hz. In the Z axis, the highest value was found for 800 Hz and it amounts to 4.

For TO, the highest RMS value can be noticed for frequencies from 800 to 900 Hz in the Y axis, where this value reaches approx. 3. A significant difference is the Z axis characterized by values exceeding the Y axis in the range of approx. 250 Hz in which the RMS value is over 3, 5. The X axis is characterized by max. 2 values for 600 Hz.

As would be expected, these values are largely analogous to the analysis of the maximum values in the FFT spectrum in the same bandpass configuration. Each of the passenger train signals is characterized by the maximum gain in the Y axis, but it is not dominant for the freight train, where the Z axis gives us a greater role in the information capacity. A correlation between all trains in the Y axis has been noticed, i.e. higher RMS values for frequency 800 Hz \pm 200 which gives the basis for further analyses. Further analysis of the commodity composition is also necessary, where an increase in RMS was also noticed at lower frequencies, especially around 200–300 Hz.

3.2 Acoustics Measurements

In order to analyze the vibroacoustic signature, analogous processing of the recorded acoustic signals was carried out. Synchronously recorded vibration and acoustic signals are the basic source and carrier of the vibroacoustic image of a passing train and the source of its vibroacoustic signature. In the initial phase of the analysis, the similarities in the phenomena and the information transmitted by vibration and acoustic signals were assumed. In order to verify these assumptions, the same signal analyzes were carried out in order to compare the separated information components.

Acoustic signal waveforms before filtering have been depicted below (Fig. 4).

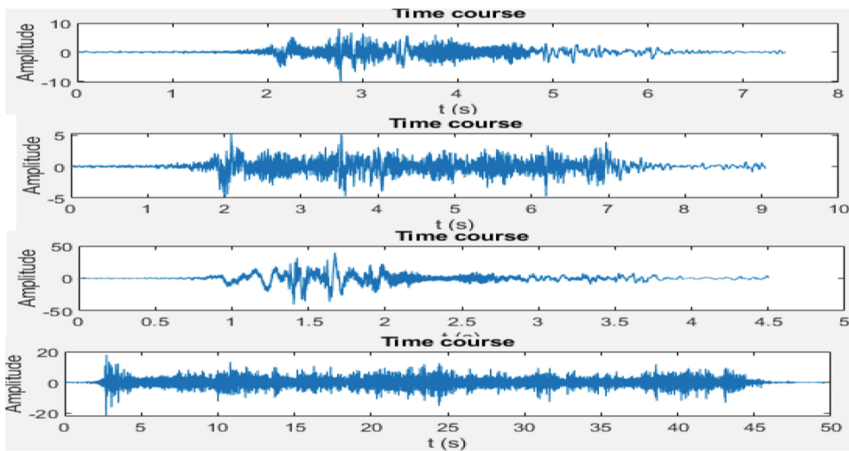


Fig. 4. Sequentially from the top, non-filtered noise waveforms of the analysed compositions with the following designations: EMU, HSR, PO, TO.

As it can be seen in the above graphic, the acoustics signal of vehicles differ significantly in various respects, similarly to the vibration analysis. This is important information for the further handling and analysis of files.

The table below shows the basic characteristics of the noise waveforms for the above-mentioned compositions (Table 2).

Table 2. Calculated RMS, Peak 2 Peak and Max values for noise waveforms before filtering.

Type	RMS	PEAK 2 PEAK	MAX value
Electric railcar (EMU)	1,051	18,49	8,044
High-speed rail (HSR)	0,765	10,19	5,290
Electric locomotive with passenger railroad cars (PO)	5,443	79,92	39,51
Electric locomotive with hopper wagons (TO)	2,337	39,97	17,90

Summary of the results after filtering, including the highest dft (f) value for a given analyzed frequency with the Bandpass filter 100–20,000 Hz every 1,000 Hz.

All compositions were characterized by low frequency in the ranges up to 4,000 Hz. This gives rise to interest and further analysis of data below this value. It is also information that the equipment used for recording does not have to meet the sampling requirements above 20,000 Hz. Further analysis of the sound in the range below 1,000 Hz is also necessary. A visible distinction is made only by PO and EMU - the gain is greater than in the other two (Figs. 5 and 6).

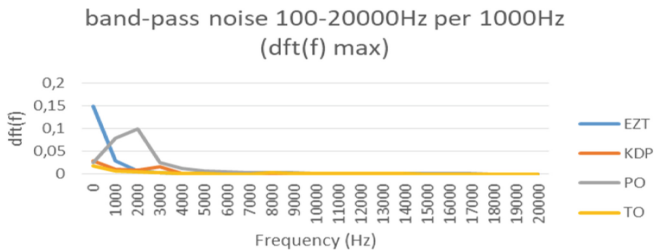


Fig. 5. Results after band-pass step method filtering in the range from 10 to 20,000 Hz in windows 1,000 Hz - the highest amplitude. Y axis - FFT gain, X axis - frequency (Hz). Diagram markings as in the figure.

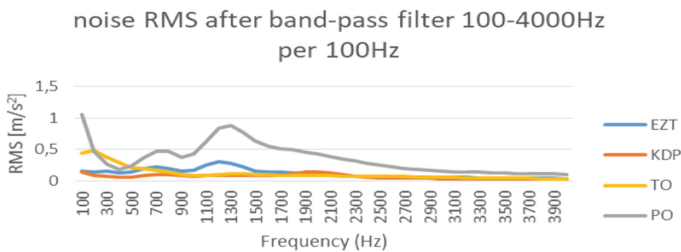


Fig. 6. Results after band-pass filtering in the range from 100 to 4,000 Hz in windows of 100 Hz - calculation of the RMS value. Diagram markings as in the figure.

The results from the RMS calculation after filtering the signals gave significant differences compared to the max dft (f) calculation. All compositions were characterized by a low frequency in the ranges up to 4,000 Hz, which was used here with a focus on lower frequencies. Due to this relationship, a band-pass step method filter was used, filtering in the 100 Hz windows than before 1,000 Hz. A significant difference can be noticed in the case of the PO composition, which, in contrast to HSR and EMU which are similar structures, i.e. EMU and HSR, is characterized by higher RMS values, in two frequency ranges, i.e. up to 300 Hz and between 1,100 and 2,500 Hz. Higher values can also be noticed in the case of the TO composition which is characterized by frequencies up to 500 Hz. From the aerodynamic point of view, the EMU and HSR trainsets are better adapted to higher speeds, therefore their values are lower than those of other structures.

4 Summary and Conclusion

The paper summarizes the extended analysis of the influence of a passing railway train on the spectrum and the course of vibrations in three axes as well as the FFT analysis. The article presents the results of tests of rail vibrations forced by the passage of a rail vehicle. For comprehensive analysis, vibrations were recorded in three axes: longitudinally, transverse and vertically. The analysis was carried out in the time domain as a distribution of vibration accelerations in successive recording periods, which allows for the identification of the torn time window. Additionally, in order to analyze the signal dynamics, frequency spectra have been defined, which allow the evaluation of the frequency components. Due to the fact that the recorded signals belong to the group of non-stationary signals, they were also transformed into the t-f representation. This allows you to observe the time distribution for specific frequency bands. Comprehensive comparison of the obtained results allows the observation of vibroacoustic images that can be treated as a trace and signature of a passing train. As a consequence, a set of data is obtained that can be analyzed according to various criteria, including assessment of the impact of vibrations and noise on means of transport. An additional assumption of the authors is the possibility of identifying railway trains only with the help of vibroacoustic signals generated by them, which according to the existing premises it is possible. An additional correlation with sound gives attitudes to the premises for the validity of such a thesis. The analyzed noise generated by passing railway trains was recorded synchronously with the vibration waveforms listed above. The analysis was performed with the use of a band-pass step method filter for vibrations at frequencies from 100 to 2,500 Hz every 100 Hz and noise for frequencies from 10 to 20,000 Hz every 1,000 Hz. In both cases, there are significant differences in the amplitude gain levels as well as in the results presented in the form of graphs with calculated max dft (f) values. In the case of noise, all trains were characterized by a low frequency (below 4,000 Hz). This gives rise to interest and further analysis of data below this value. Further analysis of the sound in the range below 1,000 Hz is also necessary. On the other hand, the analysis of vibrations may require further analyzes in the future, such as a comparison of several dozen compositions of one type and recalculation of the max dft (f) and RMS for each of them. On the other hand, the data

presented in the article reflect a well-selected research sample (the four most popular types of trains traveling on Polish tracks). The role of aerodynamic train structures (EMU and HSR) was also noticed in the case of noise analysis for RMS values.

Acknowledgement. Work presented in this study was supported by the European Union through the European Social Fund as a part of a Silesian University of Technology as a Centre of Modern Education based on research and innovation project, number of grant agreement: POWR.03.05.00 00.z098/17-00.

References

1. Burdzik, R., Słowiński, P., Juzek, M., Nowak, B., Rozmus, J.: Dependence of damage to the running surface of the railway rail on the vibroacoustic signal of a passing passenger train. *Vibroeng. Procedia* **19**, 226–229 (2018)
2. Chromański, W.: *Simulation and Optimization in the Dynamics of Rail Vehicles*, p. 141. The Publishing House of the Warsaw University of Technology, Warsaw (1999)
3. Thompson, D.: Railway noise and vibration: the use of appropriate models to solve practical problems. In: *The 21st International Congress on Sound and Vibration*, Beijing, China, 13–17 July 2014 (2014)
4. Wszolek, T., Majchrowicz, J.: Analysis of the usefulness of distinctive noise features from rail and wheel in assessing their impact on the overall railway noise level. *Diagnostyka* **20** (2019)
5. Durka, P.J.: *Between time and frequency: elements of modern signal analysis*. Faculty of Physics, University of Warsaw (2004)
6. Cisielski, R., Maciąg, E.: *Road Vibrations and their Influence on Buildings*, p. 248. Publishing House of Communication and Communications, Warsaw (1990)
7. Jeong, D., Choi, H., Choi, Y., Jeong, W.: Measuring acoustic roughness of a longitudinal railhead profile using a multi-sensor integration technique. *Sensors* **19**(7), 1610 (2019). <https://doi.org/10.3390/s19071610>
8. Nader, M.: *Vibration and Noise in Transport - Selected Issues*. Publishing House of the Warsaw University of Technology, Warsaw (2016)
9. Railway noise. Gijssjan van Blokland M+P Ard Kuijpers M+P sources: Müller-BBM (D), D. Thompson (GB), M.Dittrich (TNO). topics. Relevance Sources Rolling noise Propulsion noise Aero dynamic noise Model of generation process of rolling noise Force generation in wheel/rail contact
10. Zvolenský, P., Grenčík, J., Pultznerová, A., Kašiar, L.: Research of noise emission sources in railway transport and effective ways of their reduction. In: *MATEC Web of Conferences*, vol. 107, p. 00073 (2017)
11. Burdzik, R., Nowak, B.: Application of vibration signals in the rail vehicle identification system. In: *Diagnostyka Maszyn. XLVII Ogólnopolskie Sympozjum* (2020)
12. Burdzik, R., Nowak, B., Konieczny, Ł., Mańka, A.: Analysis of the propagation of vibration waves in the railroad rails caused by the vehicle's passage. In: *WibroTech 2019*, Zawiercie (2019)
13. Bhore, C., Andhare, A., Padole, P., Korde, M.: Analysis of track vibration for metro rail. In: Kalamkar, V.R., Monkova, K. (eds.) *Advances in Mechanical Engineering: Select Proceedings of ICAME 2020*, pp. 67–73. Springer Singapore, Singapore (2021). https://doi.org/10.1007/978-981-15-3639-7_9

14. Trimpe, F., Salander, C.: Wheel–rail adhesion during torsional vibration of driven railway wheelsets: vehicle system dynamics. *Int. J. Veh. Mech. Mobility* **59**(5), 785–799 (2020)
15. Chen, C., Fang, C., Qu, G., He, Z.: Vertical vibration modelling and vibration response analysis of Chinese high-speed train passengers at different locations of a high-speed train. *Proc. Inst. Mech. Engineers Part F J. Rail Rapid Transit* **235**, 35–46 (2020)
16. He, X., Shi, K., Wu, T.: An efficient analysis framework for high-speed train-bridge coupled vibration under non-stationary winds. *Struct. Infrastruct. Eng. Maintenance Manag. Life-Cycle Des. Perf.* **16**(9), 1326–1346 (2019)
17. Khan, M.R., Dasaka, S.M.: Characterisation of high-speed train vibrations in ground supporting ballasted railway tracks. *Transp. Infrastruct. Geotechnol.* **7**(1), 69–84 (2019). <https://doi.org/10.1007/s40515-019-00091-w>
18. Liratzakis, A., Tsompanakis, Y., Psarropoulos, P.N.: Assessment of high-speed train-induced vibrations using efficient numerical models. In: Sapountzakis, E.J., Banerjee, M., Biswas, P., Inan, E. (eds.) *Proceedings of the 14th International Conference on Vibration Problems. Lecture Notes in Mechanical Engineering*. Springer, Singapore (2021)